

Three-dimensional rotation of cells at a bipolar electrode array using a rotating electric field
Yupan Wu^{*1234}, Yuanbo Yue¹, Haohao Zhang¹, Xun Ma¹, Zhexin Zhang¹, Kemu Li¹, Yingqi Meng¹, Shaoxi Wang¹, Xuewen Wang^{2*}, Wei Huang^{2*}

¹ School of Microelectronics, Northwestern Polytechnical University, Xi'an, PR China 710072,

² Frontiers Science Center for Flexible Electronics (FSCFE) & Shaanxi Institute of Flexible Electronics (SIFE), Northwestern Polytechnical University (NPU), 127 West Youyi Road, Xi'an, 710072, China.

³ Research & Development Institute of Northwestern Polytechnical University in Shenzhen, PR China 518000

⁴ Yangtze River Delta Research Institute of NPU, Taicang, PR China 215400. ⁵ School of Engineering, Zhejiang A & F University, Hangzhou, 311300, PR China

*Corresponding author. E-mail: iamxwwang@nwpu.edu.cn, wyp721@nwpu.edu.cn, iamdirector@fudan.edu.cn

1. Theoretical background

1.1 Dielectrophoresis

Dielectrophoresis is the force exerted by a non-uniform electric field on a polarizable particle in an electrolyte. For a spherical dielectric particle, the time averaged DEP force can be written as:

$$\langle F_D \rangle = \pi r^3 \varepsilon_m \text{Re} [K(w)] \nabla (E \cdot E^*) - 2\pi r^3 \varepsilon_m \text{Im} [K(w)] (\nabla \times \text{Re} (E) \times \text{Im} (E)) \quad (1)$$

The DEP force vector depends on the degree of non-uniformity of the electric field and the magnitude of the Clausius-Mossotti factor:

$$K(w) = \left(\varepsilon_p^* - \varepsilon_m^* \right) / \left(\varepsilon_p^* + 2\varepsilon_m^* \right) \text{ with } \varepsilon^* = \varepsilon - j(\sigma/\omega). \quad (2)$$

where ε_p^* and ε_m^* denote the frequency-dependent complex permittivities of the particles and its suspending medium, ε is the permittivity of liquid, σ is the conductivity, r is the particle radius. $\text{Im}(K(w))$ and $\text{Re}(K(w))$ are the imaginary and real parts of the factor $K(w)$. The first term in Eq (1) is the conventional DEP (cDEP) force. The particle will be attracted to or propelled from the dense electric field region depending on whether $\text{Re}(K(w))$ is positive or negative. The former and the latter are termed positive DEP (pDEP) and negative DEP (nDEP) force respectively. The transition from positive to negative DEP or vice versa is called the cross-over frequency. The second term in Eq (1) denotes the traveling wave DEP (twDEP) force. Depending on the polarity of the factor $\text{Im}(K(w))$, the PS microbead will be directed towards the regions where the phases of the field component are smaller ($\text{Im}(K(w)) < 0$) or larger

($\text{Im}(K(w)) > 0$). By equating Eq (1) and the drag force, $F_D = 6\pi\eta rv$, the motion of PS microbeads or cells can be deduced.

Under a DC electric field, the DEP force depends on the relative conductivities of the particle and suspending medium: $f_{CM} = (\sigma_p - \sigma_m)/(\sigma_p + 2\sigma_m)$. The total particle conductivity is obtained by the sum of the bulk conductivity and the surface conductivity which is calculated by $\sigma_{ps} = 2K_s/a$, where K_s is the surface conductance, typically about 1 nS. $\sigma_p \approx \sigma_{ps}$.

When suspended in a rotating electric field, the cell experiences a torque Γ_{DEP} given by

$$\Gamma_{DEP} = -4\pi R^3 \epsilon_m \text{Im}[K(w)] E^2 \quad (3)$$

Assuming that the cell rotates at a constant angular velocity Ω , the hydrodynamic torque Γ_f arising from the Stokes drag force is given by

$$\Gamma_f = 8\pi\eta\Omega R^3 \quad (4)$$

where η is the viscosity of the medium.

In equilibrium, $\Gamma_{DEP} = \Gamma_f$. Combining eqn (3) and (4) we get

$$\Omega = \frac{\epsilon_m}{2\eta} \text{Im}[K(w)] E^2 \quad (5)$$

1.2 Induced charged electroosmosis

Traditional electroosmotic flows occur^[28] when an applied electric field forces the thin ionic clouds which screen charged surfaces into motion. Unlike the former, In induced charge electroosmosis (ICEO) phenomena arises when the diffuse double layer charge is induced around polarizable surfaces by an applied electric field and subsequently the same electric field drives the induced charge into motion^[29]. So, the fundamental difference is the origin of the diffuse double layer charge. In ICEO the double layers are provided by electrical conductors which may not be energized, whereas in ACEO the double layers are formed on the electrode surfaces^[30].

The standard model of ICEO encompasses the Poisson-Nernst-Planck (PNP) equations of ion transport coupled to the Navier-Stokes equations of viscous fluid flow. On the basis of the assumption of linear or weakly nonlinear charging dynamics, this model can be simplified by decoupling the electrokinetic problem into electrochemical relaxation and viscous flow.

Electrochemical relaxation. The electric potential in the fluid bulk can be achieved by solving Laplace's equation:

$$\nabla \cdot (\sigma \mathbf{E}) = -\sigma \nabla^2 \phi = 0, \quad (6)$$

assuming electrolytes with a constant conductivity σ .

A compact Stern layer is often assumed to act as a capacitor in series with diffuse layer capacitor, the total induced double layer (IDL) capacitance is $C_0 = C_s C_D / (C_s + C_D) = C_D / (1 + \delta)$, the voltage across the diffuse layer capacitor only occupies a portion of the total double layer voltage $\psi_D = \Delta\phi / (1 + \delta)$, where $C_D = \epsilon / \lambda_D$ is the capacitance of the diffuse layer, C_s is the

capacitance of the Stern layer. $\delta = C_D/C_s$ is the ratio of the diffuse layer to Stern layer capacitance, ε is the permittivity and $\lambda_D = \sqrt{D\varepsilon/\sigma} = 37.6$ nm is the Debye screening length, where $D = 2 \times 10^{-9} \text{ m}^2/\text{s}$ is the bulk diffusivity, $\varepsilon = 7.08 \times 10^{-10} \text{ F/m}$ is the permittivity.

A capacitance like boundary condition closes the equivalent RC circuit and the normal current from the bulk charges the diffuse layer:

$$C_0 \frac{d\psi_0}{dt} = -\sigma \hat{n} \cdot \nabla \phi = \sigma E_n \quad (7)$$

Using complex amplitudes, the above condition can be written as

$$j\omega C_0 \frac{\phi_0 - \phi_0^c}{1 + \delta} = \sigma \hat{n} \cdot \nabla \phi^c \quad (8)$$

where, ϕ^c is the potential in the bulk outside the IDL, ϕ_0^c is the potential at the metal surface.

The boundary condition at the insulating surface can be given by

$$\frac{\partial \phi}{\partial y} = 0 \quad (9)$$

The time averaged flow, given by the Helmholtz-Smoluchowski boundary condition for the effective slip on the polarizable surface, is

$$\langle v_s \rangle = \frac{-\varepsilon}{2\eta} \text{Re} \left(\zeta \mathbf{E}_t^* \right) = \frac{-\varepsilon}{\eta} \frac{1}{1 + \delta} \frac{1}{2} \text{Re} \left((\phi_0 - \phi_0^c) (\mathbf{E} - \mathbf{E} \cdot \mathbf{n} \cdot \mathbf{n})^* \right) \quad (10)$$

where \mathbf{E}_t is the tangential electric field, ζ is the zeta potential, η is the fluid viscosity, P is the pressure, the asterisk signifies complex conjugation.

The no slip boundary condition is applied to other insulating surface and the driving electrode surface.

$$\mathbf{v} = 0 \quad (11)$$

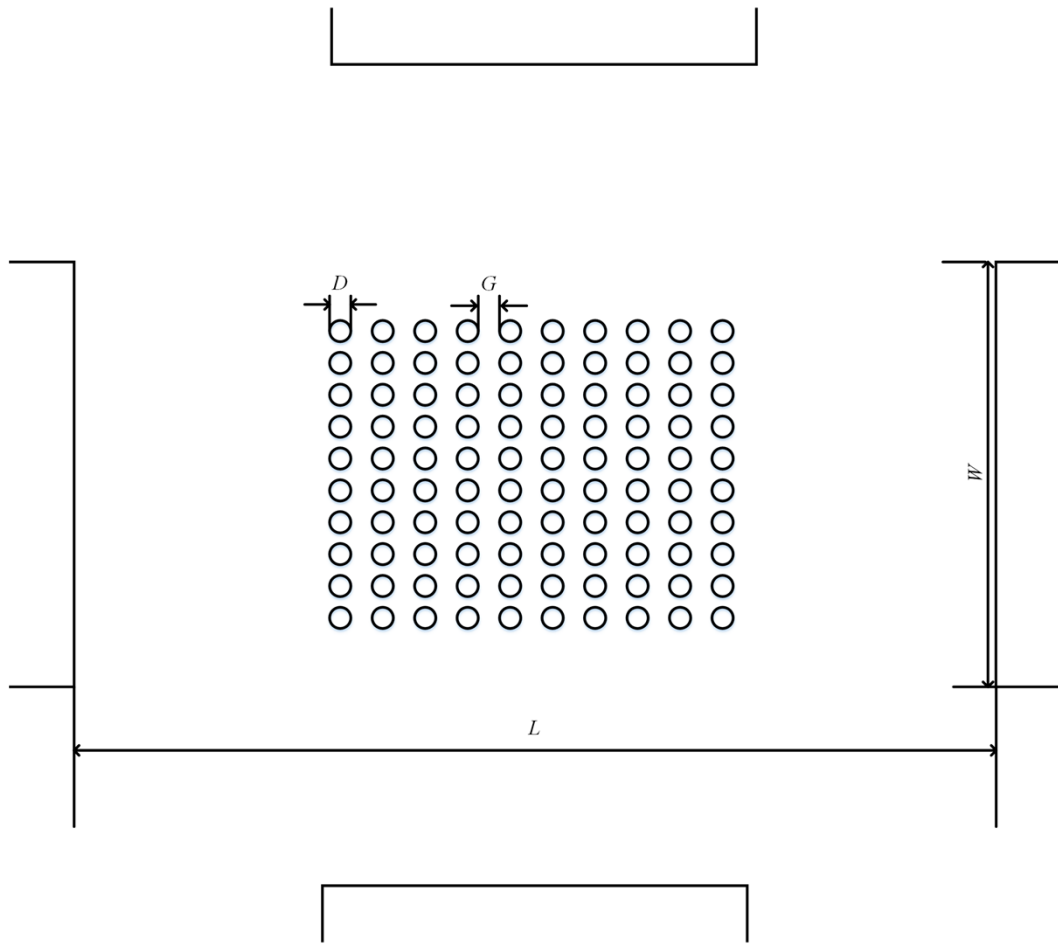


Figure S1 Top view of the microfluidic chip for 3D cell electrorotation in a static chamber.

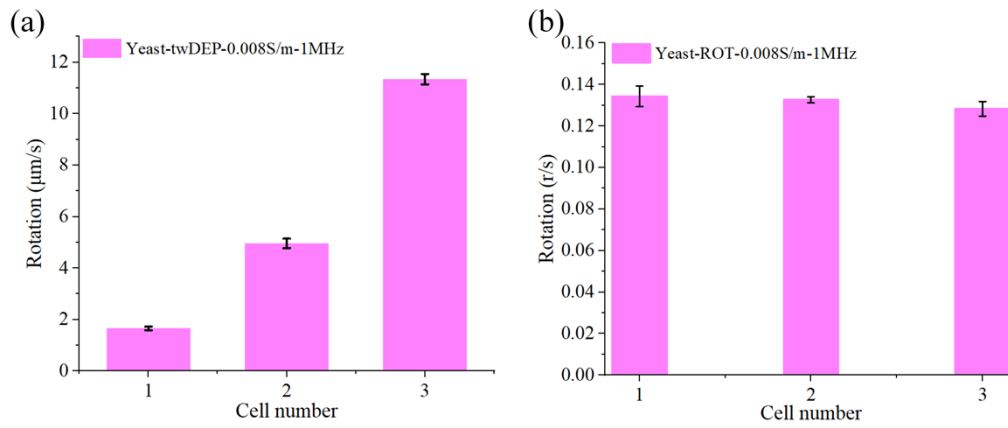


Figure S2. (a) The rotation speeds of yeast cells around the BPE at $f = 1$ MHz, $A = 10$ V in aqueous solutions with 0.008 S/m. (b) The electrorotation speeds of yeast cells at $f = 1$ MHz, $A = 10$ V in aqueous solutions with 0.008 S/m.

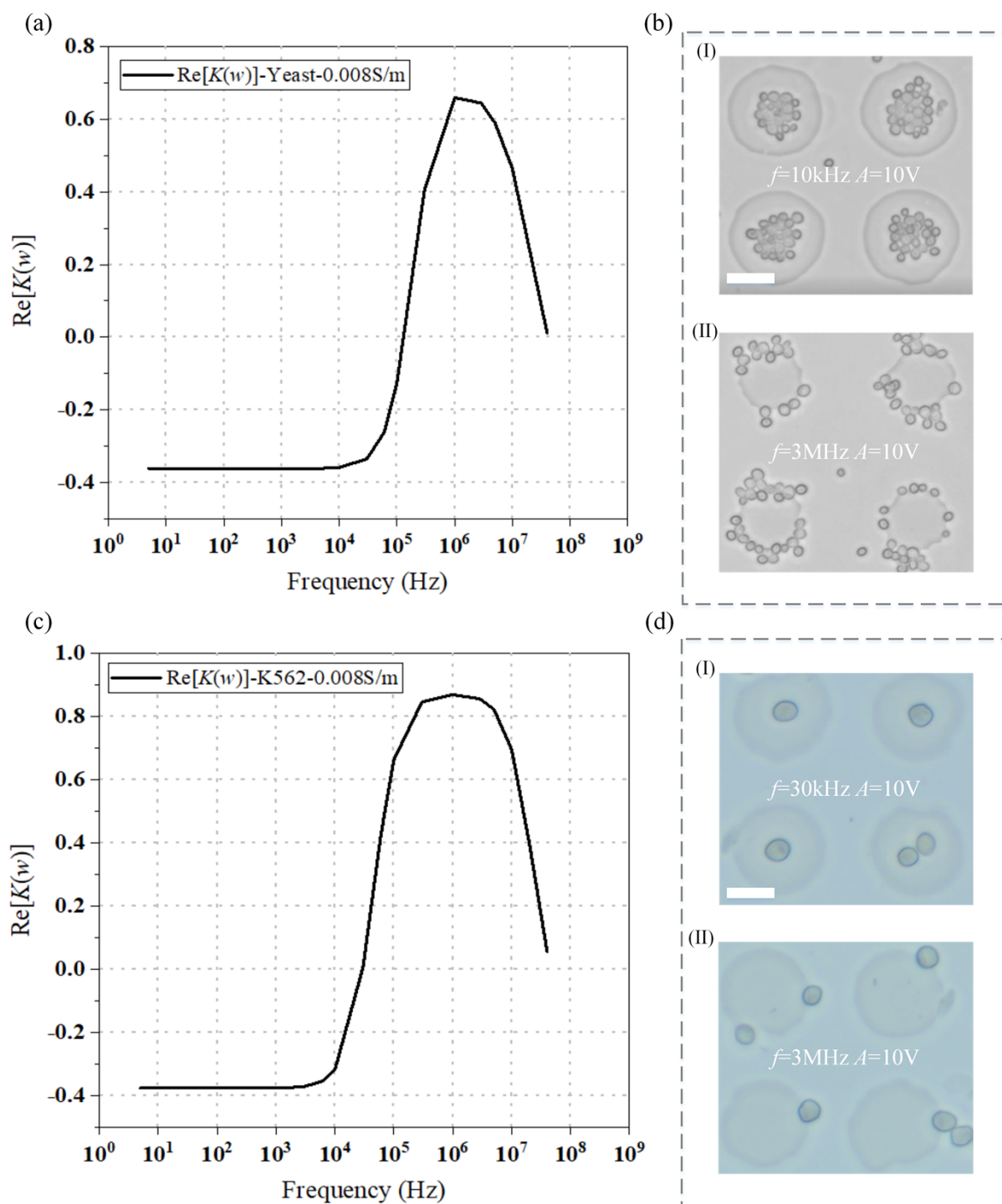


Figure S3. (a) DEP spectra of yeast cells for electrolytes with 0.008 S/m. (b) Yeast cells are driven to different locations in the bipolar electrode array. (I) Yeast cells are driven to the center of the bipolar electrode array at $f = 10$ kHz, $A = 10$ V. (II) Yeast cells are driven to the edge of the bipolar electrode array at $f = 3$ MHz, $A = 10$ V. (c) DEP spectra of K562 cells for

electrolytes with 0.008 S/m. (d) K562 cells are driven to different locations in the bipolar electrode array. (I) K562 cells are driven to the center of the bipolar electrode array at $f = 30$ kHz, $A = 10$ V. (II) K562 cells are driven to the edge of the bipolar electrode array at $f = 3$ MHz, $A = 10$ V. Scale bar, 50 μm .

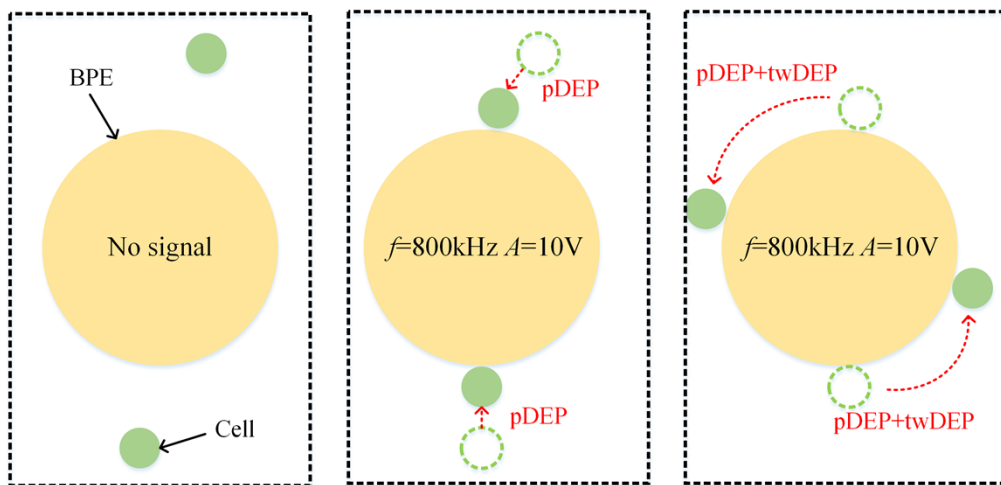


Figure S4. Flexible control of cell rotation position based on cDEP and twDEP forces.

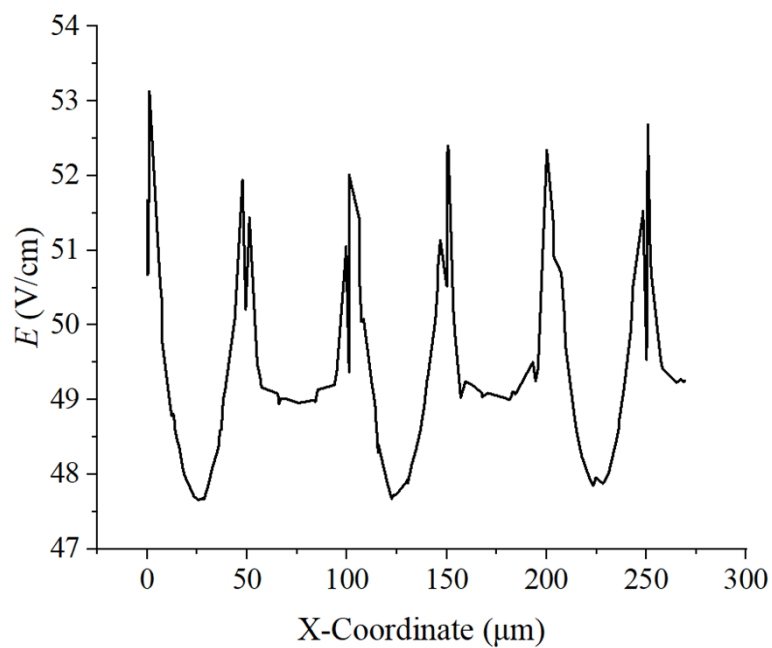


Figure S5 The field strength along the line A'-A' in Fig 1b at $A = 10$ V.

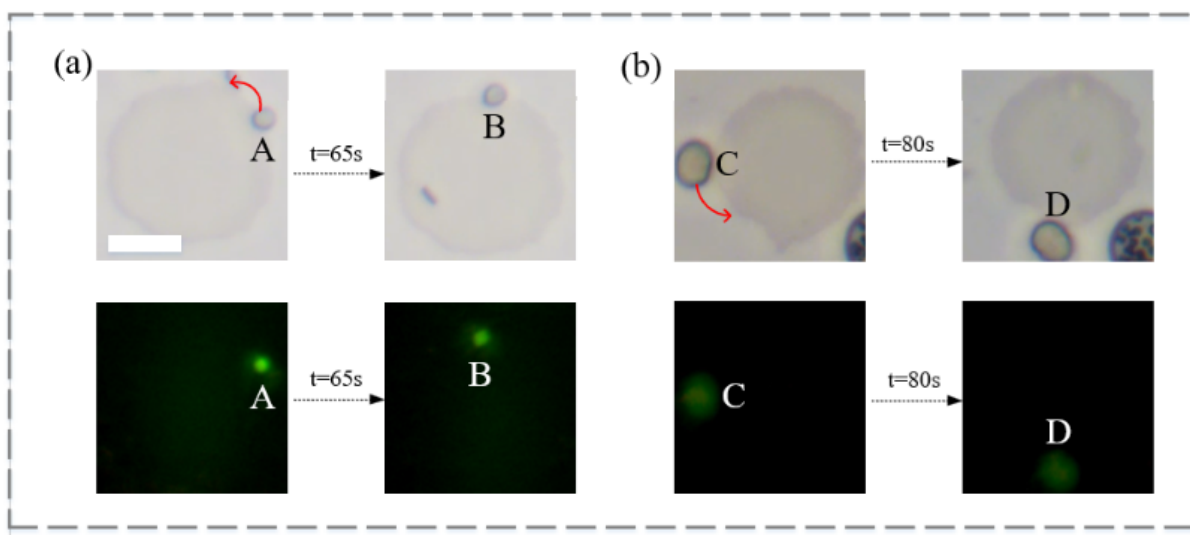


Figure S6. Yeast (a) and K562 (b) cells remain green under fluorescence

Table S1. Geometrical parameters for the structure of the proposed chip

Parameters	Value (μm)	Implication
W	1000	width of driving electrode
L	2000	the gap of the driving electrodes
D	50	diameter of bipolar electrode
G	30	the gap of each bipolar electrode

1. Gonzalez, A.; Ramos, A.; Green, N. G.; Castellanos, A.; Morgan, H., Fluid flow induced by nonuniform ac electric fields in electrolytes on microelectrodes. II. A linear double-layer analysis. *Phys Rev E Stat Phys Plasmas Fluids Relat Interdiscip Topics* **2000**, *61* (4 Pt B), 4019-28.
2. Squires, T. M., Induced-charge electrokinetics: fundamental challenges and opportunities. *Lab Chip* **2009**, *9* (17), 2477-83.
3. Harnett, C. K.; Templeton, J.; Dunphy-Guzman, K. A.; Senousy, Y. M.; Kanouff, M. P., Model based design of a microfluidic mixer driven by induced charge electroosmosis. *Lab Chip* **2008**, *8* (4), 565-72.

4. Schnelle, T.; Müller, T.; Gradl, G.; Shirley, S. G.; Fuhr, G., Paired microelectrode system: dielectrophoretic particle sorting and force calibration. *Journal of Electrostatics* **1999**, *47* (3), 121-132.
5. Wu, C.; Chen, R.; Liu, Y.; Yu, Z.; Jiang, Y.; Cheng, X., A planar dielectrophoresis-based chip for high-throughput cell pairing. *Lab Chip* **2017**, *17* (23), 4008-4014.
6. Wu, Y.; Ren, Y.; Tao, Y.; Hou, L.; Hu, Q.; Jiang, H., A novel micromixer based on the alternating current-flow field effect transistor. *Lab Chip* **2016**, *17* (1), 186-197.